Journal of Pharmaceutical and Biomedical Analysis 51 (2010) 202–209

Contents lists available at ScienceDirect

Journal of Pharmaceutical and Biomedical Analysis

journal homepage: www.elsevier.com/locate/jpba

Liquid chromatography/mass spectrometry-based structural analysis of new platycoside metabolites transformed by human intestinal bacteria

Young Wan Ha [a,b], Yun-Cheol Na [c], In Jin Ha [a], Dong-Hyun Kim [d], Yeong Shik Kim [a,*]

[a] Natural Products Research Institute, College of Pharmacy, Seoul National University, 599 Gwanangno, Gwanak-gu, Seoul 151-742, Republic of Korea
[b] Life Sciences Division, Korea Institute of Science and Technology, Seoul 136-791, Republic of Korea
[c] Korea Basic Science Institute, Seoul 136-713, Republic of Korea
[d] Department of Pharmaceutical Science, Kyung Hee University, Seoul 130-701, Republic of Korea

ARTICLE INFO

Article history:
Received 2 May 2009
Received in revised form 18 July 2009
Accepted 1 August 2009
Available online 12 August 2009

Keywords:
Platycodon grandiflorum
Platycosides
LC/ESI-MS
Intestinal bacteria
Metabolism

ABSTRACT

Platycosides, the main active constituents of Platycodi Radix, have been thoroughly studied for the characterization of their potent biological activities. However, metabolism of platycosides has not yet been characterized. A HPLC electrospray ionization-tandem mass spectrometry (LC/ESI-MS^n) approach was applied to new complex platycoside metabolites transformed by human intestinal bacteria to identify their structures and determine metabolic pathway. The molecular weights of metabolites were identified by LC/ESI-MS analysis in both positive and negative modes. Structures for the platycoside metabolites were proposed by the molecular weights and the expected enzymatic activity of intestinal microbes on platycoside. In the second step, successive LC–MS^n analysis was used to demonstrate the proposed structures. Under ESI tandem mass conditions, the sequential fragmentation patterns of $[M+Na]^+$ ions exclusively showed signals, consistent with the cleavage of glycoside bonds, rearrangement and some cross-ring cleavage, thus allowing the rapid identification of platycoside metabolites. The metabolites identified in the time-dependent metabolism experiments enable us to propose several microbial pathways for platycosides. Even though the metabolites of some platycosides may have unknown structures and low levels, the analytical tools presented in this study made it possible to obtain a rapid and complete characterization of new metabolites and their metabolism pathway in human intestinal bacteria.

1. Introduction

Platycodi Radix, the root of *Platycodon grandiflorum* A.DC, is one of the important drugs used in oriental medicine. Its main constituents are glycosides of oleanane-type triterpenes [1–5]. Pharmacological and biological properties, such as anti-inflammation, anti-tumor and anti-obesity effects, have been reported for various platycosides [4,6–11]. Platycodi Radix, which contains platycosides, is frequently utilized in clinical practice and as a dietary supplement.

Although some of saponins are hydrolyzed in the stomach by gastric juice, most of the orally administered saponins inevitably come into contact with microflora and enzymes in the alimentary tract, and may be transformed before they are absorbed from gastrointestinal tract. Therefore, many experiments focusing on the degradation of saponins *in vitro* or *in vivo* have been studied. It is known that saponins are hydrolyzed and hydrated by mild acid condition, and, in particular, are also metabolized into sequentially deglycosylated or dehydrated products by intestinal microflora *in vitro* [12–18]. Saponins are also found to be transformed to mainly deglycosylated, dehydrated or hydrated metabolites *in vivo* similar to *in vitro* studies on oral administration to animal and human [19–23]. In actuality, these previous reports showed that *in vitro* saponin metabolites by intestinal bacteria were detected in rat or human plasma [12,13,20,23–25]. Thus, it is important to understand the metabolism of saponins in intestinal bacteria, as this process may affect their bioavailability and their overall absorption and biological activities *in vivo*.

The isolation and complete structural characterization of saponin metabolites are a complicated and time-consuming task, requiring several chromatographic steps and a combination of chemical and spectroscopic techniques. Hence it must be a challenging task to perform a structural analysis on all minor metabolites. Therefore, there is a need for rapid and sensitive methods for the structural characterization of saponin metabolites transformed by human intestinal bacteria.

Recently, the structural characterization of a complex platycoside mixture was successfully performed by LC–MS/MS according to their fragmentation patterns, which were consistent with the sequential cleavage of C-3 or C-28 glycoside bonds, some cross-

* Corresponding author. Tel.: +82 2 880 2479; fax: +82 2 765 4768.
E-mail address: kims@snu.ac.kr (Y.S. Kim).

0731-7085/$ – see front matter © 2009 Elsevier B.V. All rights reserved.
doi:10.1016/j.jpba.2009.08.002

ring cleavage and rearrangement, using purified known platycoside standards in our previous studies and some papers of LC–MS^n approach have been reported on saponin metabolites in biofluids such as urine or plasma [25–28]. Due to its high sensitivity and selectivity, MS detection provides valuable structural information and allows for the structural elucidation of unknown compounds at fairly low levels, even when standard samples are not available. Thus LC–MS^n approach was widely used in metabolism research.

However, human intestinal metabolism of platycosides has not yet been characterized, in spite of their potent bioactivities. Therefore, a LC–MS^n approach is, for the first time, used for rapid structural characterization of the new complex platycoside metabolites transformed by human intestinal bacteria. In addition, the metabolic pathway of platycoside was examined in human intestinal bacteria by a time-dependent incubation study.

2. Experimental

2.1. Materials and methods

General anaerobic medium (GAM) was purchased from Nissui Pharmaceutical Co. Ltd. (Tokyo, Japan). Tryptic soy broth (TS) and other media were purchased from Difco Co. (USA). Acetonitrile, ethyl acetate, methanol, *n*-butanol and isopropanol (HPLC grade) were purchased from Fisher Scientific (Pittsburg, PA, USA) for the preparation of crude sample and isolation of platycodin D. Distilled water (NANO pure Diamond, Barnstead, USA) was used for all solutions and dilutions. Reversed-phase C_{18} resin was purchased from Merck (Darmstadt, Germany). Dried Platycodi Radix was obtained at a local market in Seoul, Korea. The platycodin D was isolated and the platycoside-enriched fraction was prepared as previously described [27].

2.2. Incubation experiments and extraction

The reaction mixture containing a playcoside fraction (100 mg) in 900 mL anaerobic diluted water treated with resasurin was anaerobically incubated with *Bacteroides* JY-6 (20 g wet weight), at 37 °C for 72 h according to the previous method [12,13]. Chemical and metabolic stabilities were also examined by the incubation of platycoside fraction without intestinal bacteria and no platycoside fraction with bacteroids under the same incubation conditions, respectively. In order to study the time-dependent metabolism, the reaction mixture containing platycodin D (50 mg) in 300 mL anaerobic diluted water was incubated with the same bacteria (10 g wet weight) at 37 °C. The reaction mixture (10 mL) was taken periodically at 0, 1, 3, 6, 12, 24, 48, and 72 h after the incubation and then frozen at −80 °C until use in the experiment. After thawing the incubated samples at a room temperature, 5 mL of ethyl acetate were added to 5 mL of the incubation samples and the ethyl acetate fractions were collected. Ten volumes of methanol were added to the above residual aqueous fractions. The mixture was centrifuged at 3000 rpm for 10 min at 15 °C. The methanol soluble supernatants were combined with the above ethyl acetate fractions and were evaporated under a nitrogen flow. The samples were dissolved with methanol and filtered through a 0.45 μm syringe filter (Type Millex-HA, Millipore, USA), and then injected onto the HPLC or the LC/MS systems as described below.

2.3. HPLC–ELSD analysis

HPLC analysis of platycosides and platycoside metabolites was carried out as previously described, with some modifications [27]. In brief, HPLC analysis of platycosides was carried out on a Hitachi L-6000 instrument (Tokyo, Japan) equipped with a Sedex 75 evaporation light scattering detector (ELSD) and SIL-9A auto injector (Shimadzu, Kyoto, Japan). A Zorbax SB-Aq C_{18} column (150 mm × 4.6 mm, 5 μm particle size) from Agilent Technologies (Palo Alto, CA, USA) was used for all separations at room temperature. The HPLC conditions were as follows: eluent A, water; eluent B, acetonitrile; gradient, 0–6 min (10–15% B), 6–50 min (15–25% B), 50–70 min (25–70% B), 70–80 min (70–100% B) and then equilibration with 10% B for 8 min at a flow of 1 mL/min. The injection volume was set to 10 μL. The ELSD was set to a probe temperature of 70 °C, a gain of 7 and the nebulizer gas nitrogen adjusted to 2.5 bar.

2.4. HPLC/ESI-MS^n analysis

Chromatographic separation of the extract by HPLC (NANOSPACE SI-2, Shiseido, Japan) was performed using a C_{18} column (150 mm × 1 mm i.d., 5 μm, Phenomenex, Torrance, CA) with a mobile phase composed of differing proportions of 5% acetonitrile (A) and 95% acetonitrile (B) in water containing 0.1% formic acid at room temperature. The gradient program was performed as described above at a flow rate of 100 μL/min. All ESI-MS^n experiments were performed on a LCQ DECA XP MS (Thermo Finnigan, San Jose, CA) equipped with an electrospray ion source. All ion trap analyzer parameters were optimized according to the manufacturer's instructions. In ESI-MS experiments, the spray voltage was 4.5 kV in positive mode and −4 kV in negative mode under N_2 sheath gas flow at 50 arbitrary units. The capillary temperature was maintained at 275 °C. Sample sizes of 2 μL were injected into the column using an autosampler. Total ion chromatograms from 150 to 2000 *m*/*z* in ESI positive and negative modes were obtained. For tandem mass spectrometry, the maximum ion injection time, activation time, and isolated ion width were set to 500, 30 ms and 2.0 μm, respectively. The collision energy with helium was set to 30% of the radio frequency (5 V) applied to the ion trap analyzer.

2.5. UPLC/ESI-QTOF-MS analysis

The UPLC/ESI-QTOF-MS analysis was performed in the Korea Basic Science Institute (Gwangju, Korea). The system consisted of an ACQUITY ultra-performance liquid chromatography (UPLC) system and an electrospray ionization quadrupole time-of-flight (QTOF) mass spectrometer (MS) (SYNAPT^{TM} High Definition Mass Spectrometry^{TM} system; Waters, Milford, MA, USA). An ACQUITY UPLC BEH C_{18} column (1.7 μm, 100 mm × 2.1 mm i.d., Waters) was used as an analytical column. The column was maintained at 40 °C. The flow rate of the mobile phase was 0.4 mL/min with mobile phase consisting of (A) 10% acetonitrile containing 0.1% formic acid and (B) 90% acetonitrile containing 0.1% formic acid. The elution gradient linearly increased from 10% B to 40% B in 5 min, then increased to 60% B in 4 min, 100% B in 3.5 min. The total running time, including the conditioning of the column to the initial conditions, was 15 min. The injection volume was 10 μL. The ESI-QTOF-MS instrument was operated in the positive ion mode using a positive electrospray ionization source. The system control and analysis of the mass spectra were performed by Waters MassLynx^{TM} software. The desolvation gas was set to a flow rate of 450 L/h at a temperature of 300 °C. The source temperature was set to 100 °C. The capillary voltage was set to 3100 V, and cone voltage was set to 30 V. All analyses were acquired using an independent reference spray via the LockSpray interference with leucine enkephalin $[M+H]^+$ ion as lock mass (*m*/*z* 556.2771) to ensure accuracy and reproducibility. The accurate masses and compositions for the platycoside metabolites were calculated using the MassLynx software.

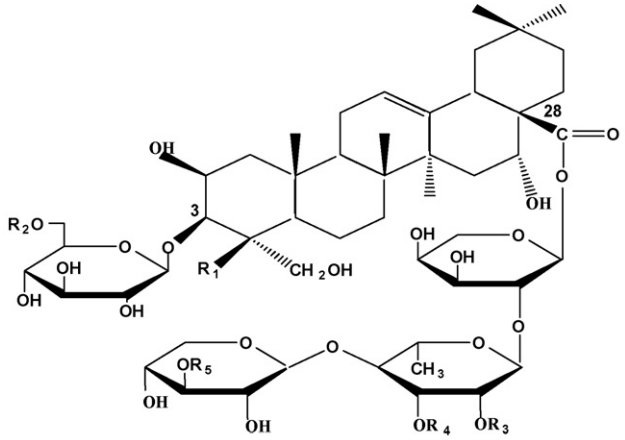

Name	Molecular formula	Molecular weight	R_1	R_2	R_3	R_4	R_5
Deapi-Platycoside E(1)	$C_{64}H_{104}O_{34}$	1416	CH_2OH	Gen	H	H	H
Platycodise E(2)	$C_{69}H_{112}O_{38}$	1548	CH_2OH	Gen	H	H	Api
Deapi-platycodin D_3(3)	$C_{58}H_{94}O_{29}$	1254	CH_2OH	Glc	H	H	H
Platycodin D_3(4)	$C_{63}H_{102}O_{33}$	1386	CH_2OH	Glc	H	H	Api
Deapi-platycodin D(5)	$C_{52}H_{84}O_{24}$	1092	CH_2OH	H	H	H	H
Platycodin D(6)	$C_{57}H_{92}O_{28}$	1224	CH_2OH	H	H	H	Api
Polygalacin D(7)	$C_{57}H_{92}O_{27}$	1208	CH_3	H	H	H	Api
3”-*O*-acetyl polygalacin D(8)	$C_{59}H_{94}O_{28}$	1250	CH_3	H	H	Ac	Api
Platycodin A(9)	$C_{59}H_{94}O_{29}$	1266	CH_2OH	H	Ac	H	Api
2”-*O*-acetyl polygalacin D(10)	$C_{59}H_{94}O_{28}$	1250	CH_3	H	Ac	H	Api

Fig. 1. Structure of platycosides from Platycodi Radix. Gen: β-D-glucose–^{6}β-D-glucose-; Glc: β-D-glucose; Api: β-D-apiose (furanose); Ac: acetyl.

3. Results and discussion

3.1. HPLC–ELSD analysis

In this study, the enriched platycoside fraction containing 10 previously identified saponin structures [27] from Platycodi Radix was used to characterize platycoside metabolites transformed by human intestinal bacteria (Fig. 1).

Firstly, the change in platycosides due to fermentation with intestinal microbes was determined by HPLC. After fermentation, the peaks of platycosides were completely transformed to the unknown peaks, which may be their metabolites converted by intestinal microbes (Fig. 2). This result indicates that the platycoside metabolites have less polar properties than platycosides due to increase of their retention times in a reversed-phase C_{18} column. The platycoside fraction was incubated without intestinal bacteria for 72 h to measure the stabilities of platycosides and blank sample, which means platycoside-free, were also tested under the same incubation conditions. These results showed that the platycosides were not altered during the incubation, and the peaks derived from blank sample were not overlapped with peaks emerged when platycosides were incubated with intestinal bacteria (see supplementary Figure S-1). These metabolites were used for subsequent structural determination by LC–ESI tandem mass analysis.

3.2. Structural determination of platycoside metabolites by HPLC/ESI-MS^n

In previous reports, the enzymatic reactions of the intestinal bacterial on saponins were presented as mainly glycoside hydrolysis, dehydroxylation and double bond reduction [12,13,18,24]. In this study, the following assignment strategy was used to obtain structural information on the novel metabolites. First, the molecular weights of metabolites were identified by LC/ESI-MS analysis in both positive and negative modes. Structures for the platycoside metabolites were proposed by the molecular weights and the expected enzymatic activity of intestinal microbes on platycoside. In the second step, successive LC–MS^n analysis was used to demonstrate the proposed structures.

In general, direct ESI-MS enabled the determination of the molecular weights of major components in crude samples. However, isomeric compounds could not be discriminated, and constituents present at low levels were unidentifiable, so an online combination of LC with ESI-MS was employed for the analysis of platycoside metabolites transformed by human intestinal bacteria. Under chromatographic conditions, 11 major peaks were detected in the extracts of platycoside metabolites (Fig. 3).

In the present experiment, metabolite 5 (M5) was selected as an example of the detailed fragmentation patterns in the successive MS experiments that were performed for the stepwise elucidation of the molecular structure. The fragmentation patterns of the other metabolites were then compared with that of M5 to obtain characteristic fragments, which can be used in the structural determination.

3.3. HPLC/ESI-MS

The molecular weight of the analyte was confirmed by ESI-MS, comparing it with predominantly $[M+Na]^+$ ion or $[M+H]^+$ ion in the positive mode and $[M-H]^-$ ion in the negative mode. Positive and negative ESI-MS analyses of M5 in LC effluent are shown in Fig. 4. However, the ESI-MS spectrum of M5 did not determine the molecular weight, because the ambiguous ion intensities in the positive mode. After introducing alkali metal ions, $[M+adduct]^+$ ions became the dominant ions for all the saponins, and the signal-to-

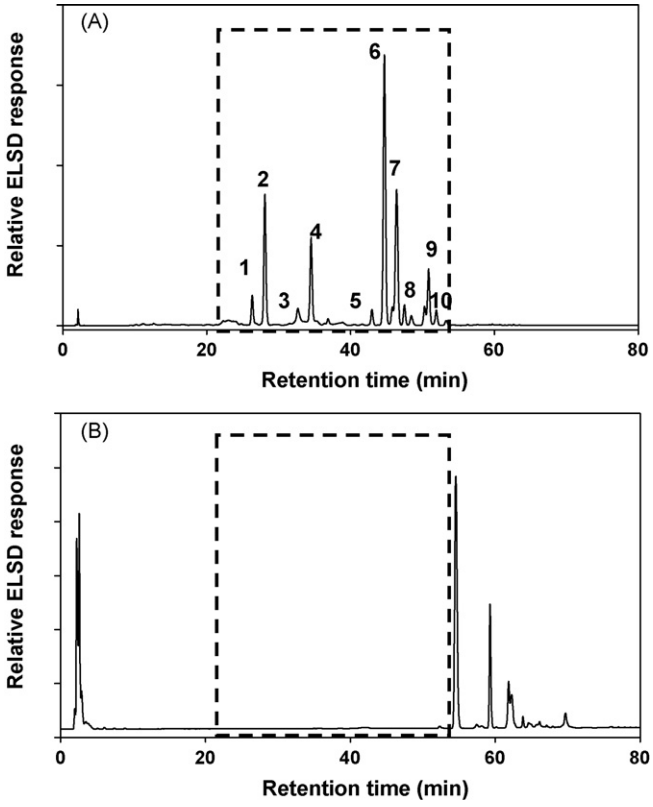

Fig. 2. Representative HPLC chromatograms of the platycoside-enriched fraction (A) and extract of platycoside metabolites transformed by human intestinal bacteria (B): Agilent Zorbax SB-Aq C_{18} column (150 mm × 4.6 mm, 5.0 μm), detector: ELSD, drift tube temperature: 70 °C, nitrogen flow rate: 2.5 bar. The numbers indicate each platycoside in Fig. 1.

noise was greatly increased [29,30]. Thus, sodium acetate (5 μM) was added to the mobile phase to enhance the sodiated molecular ion intensity, and then the significantly increased $[M+Na]^+$ ion at *m/z* 1069.4 was presented in the spectrum of ESI-MS. A high abundance of $[M-H]^-$ at *m/z* 1045.5 is observed in the negative mode. A

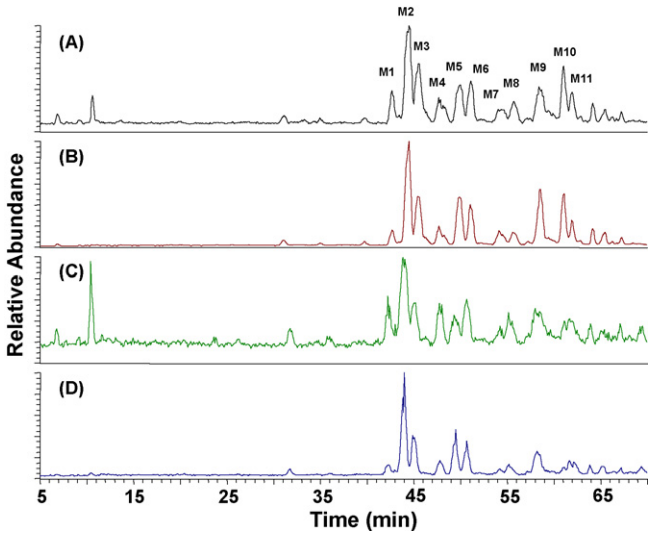

Fig. 3. Representative LC–MS chromatograms of the extract of platycoside metabolites transformed by human intestinal microbial in full scan positive and negative ion modes (acquired range *m/z* 150–2000). (A) Positive ion mode; (B) negative ion mode; (C) positive ion mode in sodium acetate added to mobile phase; (D) negative ion mode in sodium acetate added to mobile phase.

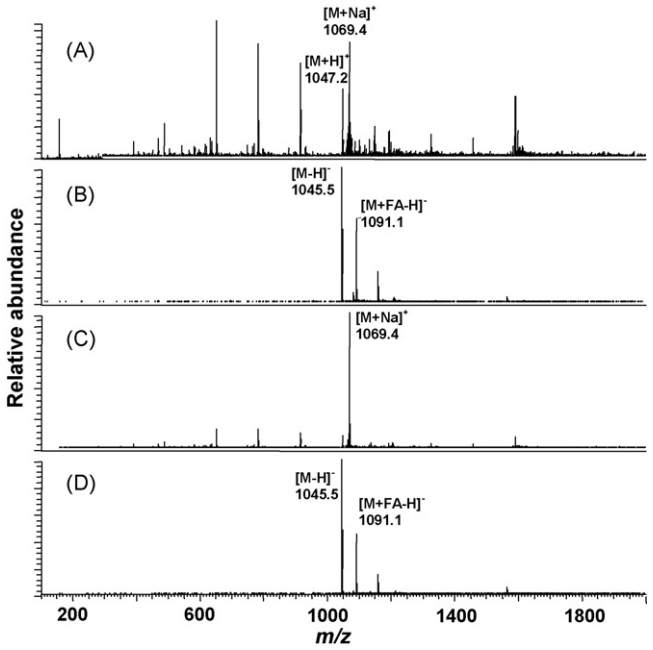

Fig. 4. ESI mass spectra of the metabolite 5 in positive and negative ion modes. (A) Positive ion mode; (B) negative ion mode; (C) positive ion mode in sodium acetate added to mobile phase; (D) negative ion mode in sodium acetate added to mobile phase.

comparison of these two spectra, with the 24 Da mass differences between the two ions, provides clear information on the molecular weight of the metabolite (1046 Da for M5). With the molecular weight determined, the structure of M5 was proposed and presented in Figs. 4 and 5. The $[M+Na]^+$ ions dominated in the positive ESI-MS spectra of all the other metabolites studied.

3.4. HPLC/ESI-MS^n

HPLC/ESI-MS^n experiments were performed for further insight into the correlation between the fragmentation patterns and structural features of this proposed metabolite. To describe the fragmentations observed in the product ion spectra of these metabolites, the fragment nomenclature proposed by Domon and Costello [31] was adopted. The ESI-MS/MS of platycoside M5 was performed in the positive and negative ion modes with $[M+Na]^+$ ions and $[M-H]^-$ ions, respectively. Only product ions ($[M-H]^-$) appeared in the negative ion mode, while more MS^n fragmentation ions were acquired in the positive ion mode. Thus, the determinations and elucidations of the fragmentation characteristics are confined to the positive mode. Fig. 5 shows the ESI-MS/MS spectrum of the $[M+Na]^+$ ion at *m/z* 1069.4 for M5. In this figure, the most abundant product ion is observed at *m/z* 565.2 $[B_0+Na]^+$, corresponding to the all sugar residues linked to C-28, and a minor peak is observed at *m/z* 433.1, corresponding to the fragment B_1. In addition, there are four Y cleavage product ions at *m/z* 937.5 (Y_3 + Na), 805.4 (Y_2 + Na), 659.3 (Y_1 + Na) and 547.3 (Y_0 + Na), which represent the loss of apiosyl, xylosyl, rhamnosyl and arabinosyl sugars attached at C-28 of triterpene, respectively, and sequentially. These results provide information on the composition and sequence of oligosaccharides linked to an aglycone at C-28. The fragment ions with low abundance at *m/z* 1025.5 $[M-CO_2+Na]^+$ and 583.2 $[B_0+H_2O+Na]^+$ can be explained by the loss of carbon dioxide and release of C-28 oligosaccharides in the rearrangement mechanism, respectively [32,33]. These unique product ions are observed in the structure, which has an oligosaccharide at C-28 and a hydroxyl group at C-16.

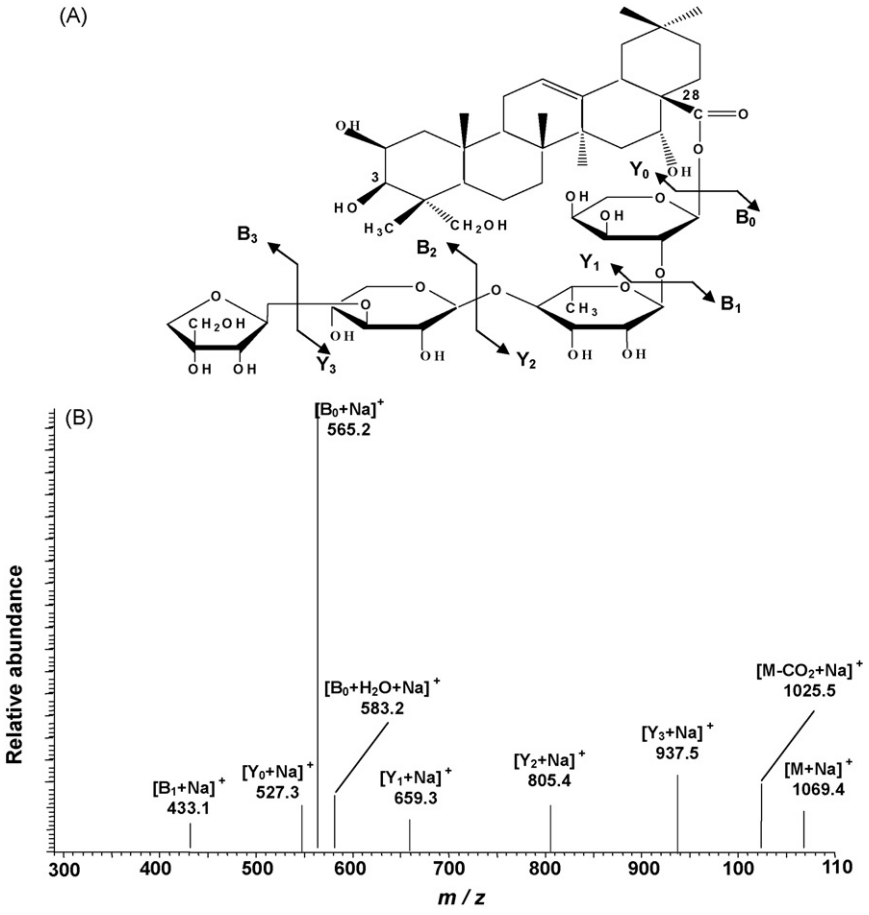

Fig. 5. Fragmentation pattern of the $[M+Na]^+$ ion of metabolite 5 (A), and ESI-MS/MS spectrum of the *m/z* 1069.4 ion ($[M+Na]^+$) of metabolite 5 (B).

To more demonstrate the structure in detail, each of the sodiated fragments at *m/z* 1025.5, 937.5, 583.2, 565.2 and 527.3 in MS/MS was selected and analyzed by ESI-MS^3 in separate experiments. The MS^3 spectrum of *m/z* 1025.5 showed a dominant ion at *m/z* 583.1 $[B_0+H_2O+Na]^+$, but $[B_0+Na]^+$ ion is not detected (Fig. 6A). It is also supported that the precursor ion at *m/z* 1025.5 is produced by the loss of carbon dioxide in the rearrangement mechanism. The minor ion at *m/z* 493.2 related to the loss of 90 Da can be produced by ring-cross cleavages of the 0, 2 two bond in arabinose ($^{0,2}X_{0\alpha}$). The spectrum (Fig. 6B) from the precursor ion $[Y_3+Na]^+$ shows peaks at *m/z* 893.3 $[Y_3-CO_2+Na]^+$, 805.4 $[Y_2+Na]^+$, 659.3 $[Y_1+Na]^+$, 527.2 $[Y_0+Na]^+$, 451.2 $[B_0-apiose+H_2O+Na]^+$ and 433.1 $[B_0-apiose+Na]^+$, with a fragmentation pattern similar to that of the MS^2 spectrum. Fig. 6C shows the MS^3 spectrum of the *m/z* 583.1 $[B_0+H_2O+Na]^+$. There are several fragments produced by cleavage of glycosidc linkages in the oligosaccharide. The ion at *m/z* 451.3 is formed after a loss of apiose and the ion at *m/z* 433.1 corresponded to $[B_1+Na]^+$ formed by loss of arabinose. The further cleavage also produced *m/z* 319.2 ion by loss of the apiose-xylose disaccharide. The other main fragment, at *m/z* 493.1, was presented by same fragmentation as described for the precursor ion at *m/z* 1025.5. The spectrum (Fig. 6D) from the precursor ion $[B_0+Na]^+$ shows peaks at *m/z* 433.1 $[B_0-apiose+Na]^+$ and 301.1 $[B_0-apiose-xylose+Na]^+$. In comparison with $[B_0+H_2O+Na]^+$, the product ion of ring-cross cleavages of the 0, 2 two bond in arabinose was not detected for the precursor ion $[B_0+Na]^+$. The reason for this result may be the double bond between C-1 and C-2 of arabinose, which forms after B_0 fragmentation. The MS^3 spectrum from $[Y_0+Na]^+$ at *m/z* 527.3 did not show any of the fragment ions.

3.5. Comparison of characteristic ions of the investigated platycoside metabolites

The structural differences among eleven platycoside metabolites transformed by *Bacteroids* JY-6, a human intestinal bacterium, were analyzed in the positive ion modes as the same manner of M5. These results are summarized and presented in Fig. 7. All the major Y ions resulting from a glycosidic bond cleavage and the expected structural features of platycoside metabolites were clearly distinguishable in the resulting fragmentation data. Therefore, the proposed structures of platycoside metabolites transformed by human intestinal bacteria are listed in Fig. 7. Fragment ions observed in MS^2 and MS^3 spectra of 11 platycoside metabolites in ESI positive ion mode are presented (see supplementary Table S-1).

3.6. Confirmation by UPLC/ESI-QTOF-MS

The UPLC/ESI-QTOF-MS system was applied to determine accurate masses of the proposed platycoside metabolites. The accurate mass data of protonated molecules were processed through the MassLynx software, which provided elemental formula, the mass errors (i.e. differences between measured masses and the calculated masses), and i-FIT (or isotope pattern fit); lower i-FIT values represent a better fit to the isotope pattern (see supplementary Figure S-2). Table 1 shows the exact mass measurements, mass errors and i-FITs obtained for the protonated molecules. For all compounds, the errors obtained were less than 5 ppm in absolute value, which is the limit of accuracy threshold except for M9.

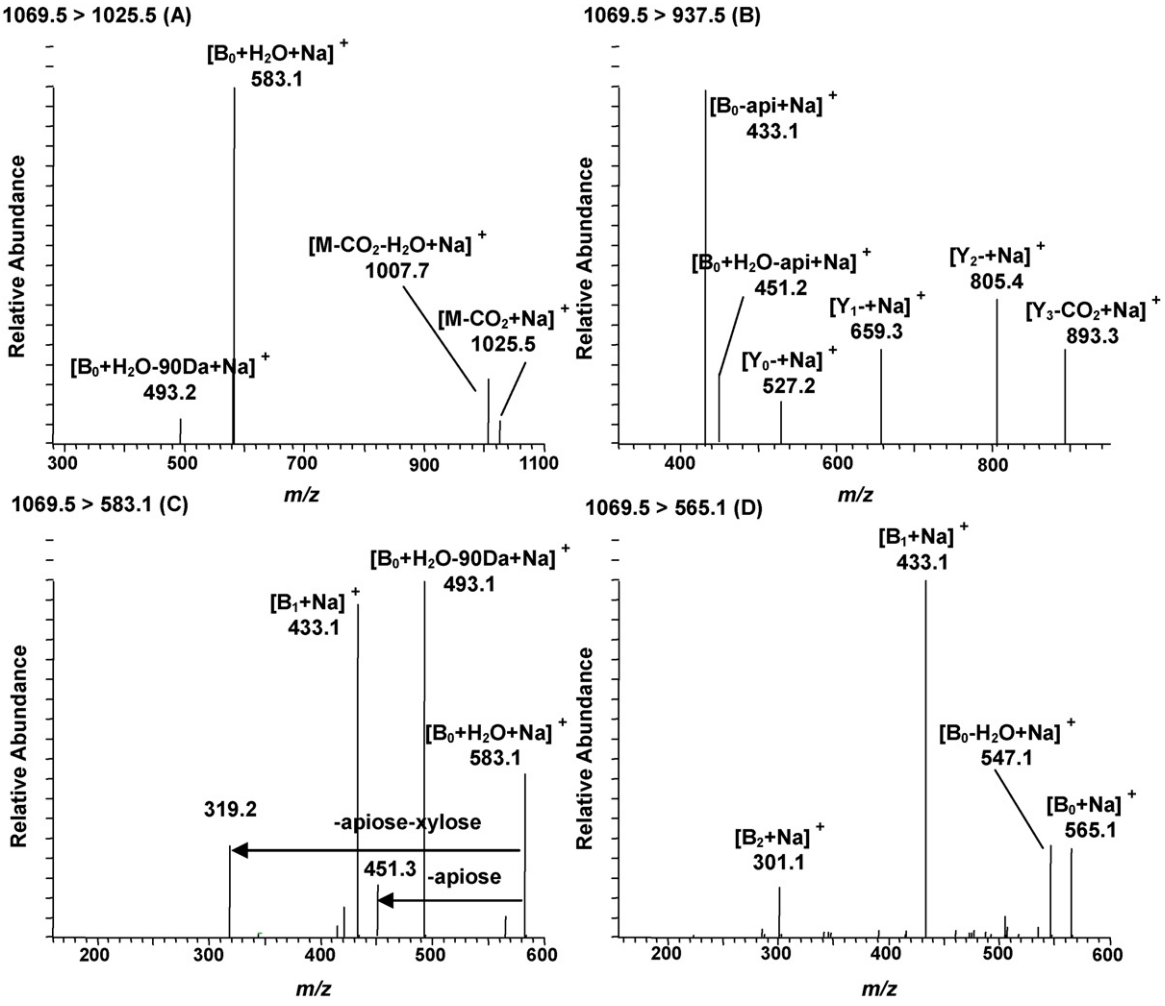

Fig. 6. Positive ESI-MS^3 spectra for metabolite 5. Precursor ion (A) $[M-CO_2+Na]^+$, (B) $[Y_3-CO_2+Na]^+$, (C) $[B_0+H_2O+Na]^+$ and (D) $[B_0+Na]^+$. Api: β-D-apiose (furanose).

3.7. Time-dependent metabolism of platycodin D

To establish the metabolism pathway of platycosides in the human intestine, time-dependent incubation experiments were performed with platycodin D, which is a major platycoside in Platycodi Radix. Based on the structures of the platycodin D metabolites and the time-dependent experiments monitored by LC/ESI-MS, a possible metabolic pathway was proposed in Fig. 8.

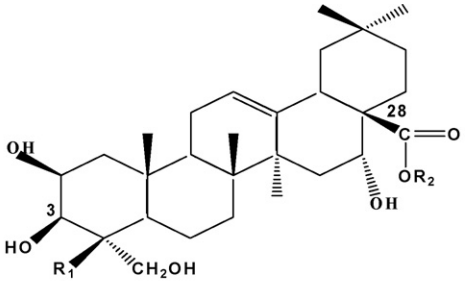

Metabolites	$[M+Na]^+$	$[Y_3+Na]^+$	$[Y_2+Na]^+$	$[Y_1+Na]^+$	$[Y_0+Na]^+$	$[B_0+Na]^+$	R_1	R_2
1	821.4	-	-	675.2	543.3	301.1	CH_2OH	-Ara-Rha
2	675.3	-	-	-	543.3	-	CH_2OH	-Ara
3	1085.4	953.3	821.2	675.3	543.4	565.1	CH_2OH	-Ara-Rha-Xyl-Api
4	805.3	-	-	659.7	527.3	301.1	CH_3	-Ara-Rha
5	1069.5	937.5	805.4	659.3	527.3	565.2	CH_3	-Ara-Rha-Xyl-Api
6	659.3	-	-	-	527.2	-	CH_3	-Ara
7, 10	1127.5	995.2	863.4	717.3	543.3	607.1	CH_2OH	-Ara+Ac-Rha-Xyl-Api
8	1127.5	995.2	863.1	675.4	543.4	607.1	CH_2OH	-Ara-Rha+Ac-Xyl-Api
9	543.3	-	-	-	-	-	CH_2OH	H
11	1127.5	995.3	863.1	717.4	585.4	565.1	CH_2OH	-Ara-Rha-Xyl-Api (Aglycone + Ac)

Fig. 7. Characteristic fragment ions observed by positive ion ESI-MS/MS analysis of platycoside metabolites (*m*/*z* values) and proposed structure of platycoside metabolites transformed by human intestinal bacterial. Rha, α-L-rhamnose (pyranose); Ara, α-L-arabinose (pyranose); Xyl, β-D-xylose; Api, β-D-apiose (furanose); Ac, acetyl.

Table 1
Accurate mass measurements of protonated molecules of platycoside metabolites transformed by human intestinal microbial.

Metabolites	Elemental composition $[M+H]^+$	Experimental mass (m/z)	Calculated mass (m/z)	Error (ppm)	i-FIT
1	$C_{41}H_{67}O_{15}$	799.4484	799.4480	0.5	29.1
2	$C_{35}H_{57}O_{11}$	653.3932	653.3901	4.7	49.3
3	$C_{51}H_{83}O_{23}$	1063.5354	1063.5325	2.7	45.5
4	$C_{41}H_{67}O_{14}$	783.4529	783.4531	−0.3	47.0
5	$C_{51}H_{83}O_{22}$	1047.5392	1047.5376	1.5	8.0
6	$C_{35}H_{57}O_{10}$	637.3944	637.3952	−1.3	0.6
7	$C_{53}H_{85}O_{24}$	1105.5469	1105.5431	3.4	43.7
8	$C_{53}H_{85}O_{24}$	1105.5446	1105.5431	1.4	36.6
9	$C_{30}H_{47}O_7$	519.3357	519.3322	6.7	43.5
10	$C_{53}H_{85}O_{24}$	1105.5453	1105.5431	2.0	1.9
11	$C_{53}H_{85}O_{24}$	1105.5439	1105.5431	0.7	1.9

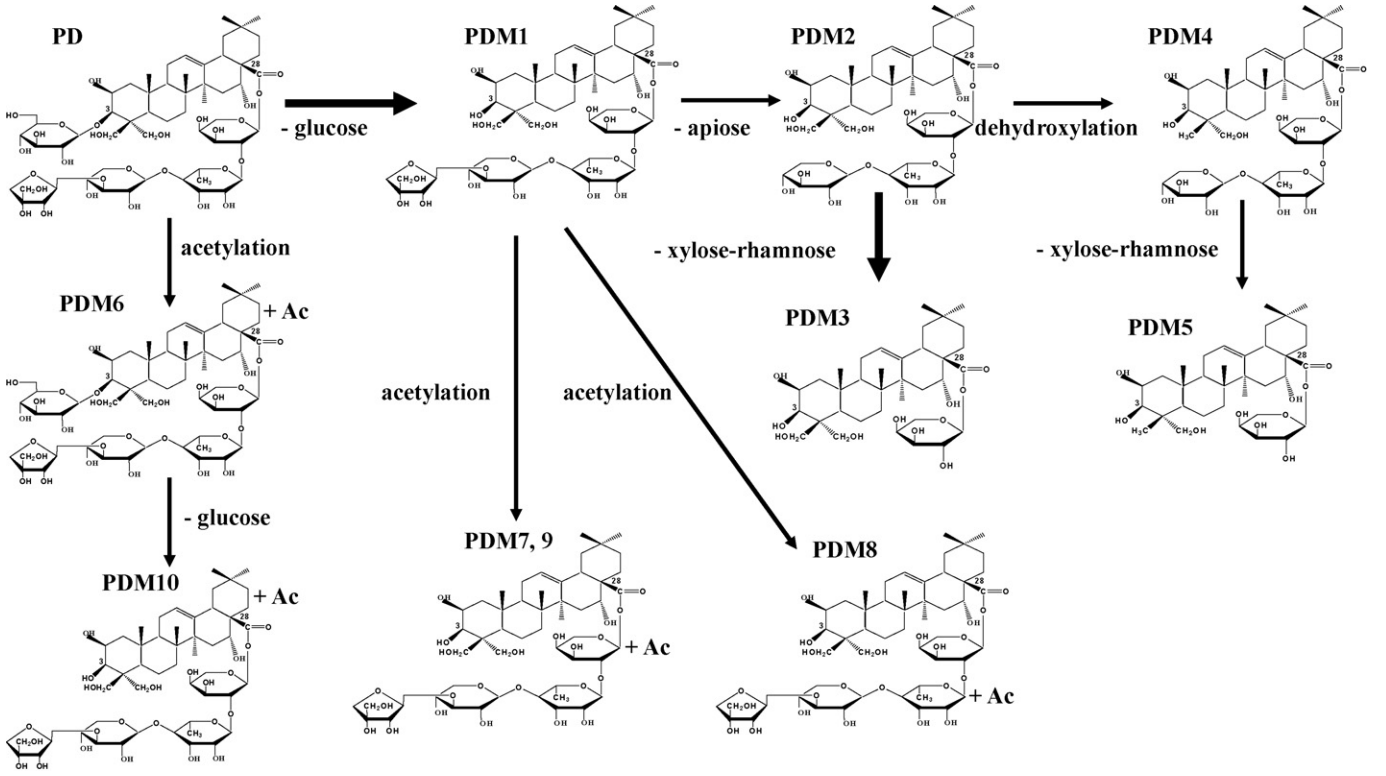

Fig. 8. Proposed metabolic pathways of platycodin D by human intestinal microbial. PD: platycodin D and PDM: platycodin D metabolite.

The deglucose-platycodin D was detected in the intestinal microbial treatment after 1 h incubation. This observation suggests that the first step in platycodin D metabolism is the hydrolysis of C-3 glycoside to aglycone, a major metabolic pathway that is terminated within 24 h (under the given conditions). This suggestion is consistent with above detected structures of all platycoside metabolites resulting from the incubation of enriched platycoside fraction with intestinal bacteria. Second, the acetylation to a hydroxyl group of aglycone, arabinose and rhamnose may occur with a rate-limiting reaction, which is then resistant to further transformation, because the results show that the ratios of these acetylated metabolites in the total metabolites are almost consistent during the 72 h incubation. Third, the metabolites resulting from the sequential cleavage of C-28 oligosaccharide and dehydroxylation of aglycone are produced by intestinal bacterial reactions (see supplementary Figure S-3).

The metabolites identified in these studies have enabled us to propose several microbial pathways for platycodin D, which is a representative constituent of platycosides, although our metabolite identification process was subject to some limitations, such as an accurate acetylation reaction site whether *O*-acetylation is at arabinose C-3 or C-4 position in M7 and M10. The major pathway of the microbial metabolism of platycodin D is the hydrolysis of C-3 glycoside, followed by acetylation at the multi-site or, alternatively, further hydrolysis at the C-28 oligosaccharide and dehydroxylation of the alglycone part.

4. Conclusions

In conclusion, a HPLC/ESI tandem mass approach was applied to the complex platycoside metabolites transformed by human intestinal bacteria. Under chromatographic conditions, eleven major peaks were detected in the extract of platycoside metabolites. Comparison of spectra in the positive and negative ion modes, with sodium acetate added to the mobile phase, provided clear information on the molecular weights of the metabolites. Under ESI tandem mass conditions, the sequential fragmentation patterns of $[M+Na]^+$ ions show exclusive signals consistent with cleavage of glycoside bonds, rearrangement and some cross-ring cleavage, thus allowing the rapid identification of platycoside metabolites transformed by human intestinal bacteria. The metabolites identified in the time-dependent experiments enable us to propose several

microbial pathways for platycodin D, although there are some limitations to the metabolite identification process, such as an accurate acetylation site.

Acknowledgement

This study was supported by a grant of the Korea Healthcare Technology R&D Project, Ministry of Health, Welfare & Family Affairs, Republic of Korea (A080974).

Appendix A. Supplementary data

Supplementary data associated with this article can be found, in the online version, at doi:10.1016/j.jpba.2009.08.002.

References

[1] W.W. Fu, N. Shimizu, D.Q. Dou, T. Takeda, R. Fu, Y.H. Pei, Y.J. Chen, Five new triterpenoid saponins from the roots of *Platycodon grandiflorum*, Chem. Pharm. Bull. (Tokyo) 54 (2006) 557–560.
[2] W.W. Fu, N. Shimizu, T. Takeda, D.Q. Dou, B. Chen, Y.H. Pei, Y.J. Chen, New A-ring lactone triterpenoid saponins from the roots of *Platycodon grandiflorum*, Chem. Pharm. Bull. (Tokyo) 54 (2006) 1285–1287.
[3] H. Ishii, K. Tori, T. Tozyo, Y. Yoshimura, Saponins from roots of *Platycodon grandiflorum*. Part 2. Isolation and structure of new triterpene glycosides, J. Chem. Soc. Perkin Trans. I (1984) 661–668.
[4] Y.S. Kim, J.S. Kim, S.U. Choi, H.S. Lee, S.H. Roh, Y.C. Jeong, Y.K. Kim, S.Y. Ryu, Isolation of a new saponin and cytotoxic effect of saponins from the root of *Platycodon grandiflorum* on human tumor cell lines, Planta Med. 71 (2005) 566–568.
[5] T. Nikaido, K. Koike, K. Mitsunaga, T. Saeki, Two new triterpenoid saponins from *Platycodon grandiflorum*, Chem. Pharm. Bull. (Tokyo) 47 (1999) 903–904.
[6] K.S. Ahn, E.J. Noh, H.L. Zhao, S.H. Jung, S.S. Kang, Y.S. Kim, Inhibition of inducible nitric oxide synthase and cyclooxygenase II by *Platycodon grandiflorum* saponins via suppression of nuclear factor-kappaB activation in RAW 264.7 cells, Life Sci. 76 (2005) 2315–2328.
[7] L.K. Han, Y.N. Zheng, B.J. Xu, H. Okuda, Y. Kimura, Saponins from platycodi radix ameliorate high fat diet-induced obesity in mice, J. Nutr. 132 (2002) 2241–2245.
[8] J.Y. Kim, Y.P. Hwang, D.H. Kim, E.H. Han, Y.C. Chung, S.H. Roh, H.G. Jeong, Inhibitory effect of the saponins derived from roots of *Platycodon grandiflorum* on carrageenan-induced inflammation, Biosci. Biotechnol. Biochem. 70 (2006) 858–864.
[9] K.J. Lee, C.Y. Choi, Y.C. Chung, Y.S. Kim, S.Y. Ryu, S.H. Roh, H.G. Jeong, Protective effect of saponins derived from roots of *Platycodon grandiflorum* on tert-butyl hydroperoxide-induced oxidative hepatotoxicity, Toxicol. Lett. 147 (2004) 271–282.
[10] C.Y. Shin, W.J. Lee, E.B. Lee, E.Y. Choi, K.H. Ko, D. Platycodin, D3 increase airway mucin release in vivo and in vitro in rats and hamsters, Planta Med. 68 (2002) 221–225.
[11] C. Wang, G.B. Schuller Levis, E.B. Lee, W.R. Levis, D.W. Lee, B.S. Kim, S.Y. Park, E. Park, Platycodin D and D3 isolated from the root of *Platycodon grandiflorum* modulate the production of nitric oxide and secretion of TNF-alpha in activated RAW 264.7 cells, Int. Immunopharmacol. 4 (2004) 1039–1049.
[12] E.A. Bae, M.J. Han, M.K. Choo, S.Y. Park, D.H. Kim, Metabolism of 20(S)- and 20(R)-ginsenoside Rg3 by human intestinal bacteria and its relation to in vitro biological activities, Biol. Pharm. Bull. 25 (2002) 58–63.
[13] E.A. Bae, J.E. Shin, D.H. Kim, Metabolism of ginsenoside Re by human intestinal microflora and its estrogenic effect, Biol. Pharm. Bull. 28 (2005) 1903–1908.
[14] G.T. Chen, M. Yang, Y. Song, Z.Q. Lu, J.Q. Zhang, H.L. Huang, L.J. Wu, D.A. Guo, Microbial transformation of ginsenoside Rb(1) by *Acremonium strictum*, Appl. Microbiol. Biotechnol. 77 (2008) 1345–1350.
[15] B.H. Han, M.H. Park, Y.N. Han, L.K. Woo, U. Sankawa, S. Yahara, O. Tanaka, Degradation of ginseng saponins under mild acidic conditions, Planta Med. 44 (1982) 146–149.
[16] M. Karikura, T. Miyase, H. Tanizawa, T. Taniyama, Y. Takino, Studies on absorption, distribution, excretion and metabolism of ginseng saponins. VI. The decomposition products of ginsenoside Rb2 in the stomach of rats, Chem. Pharm. Bull. (Tokyo) 39 (1991) 400–404.
[17] K. Kobashi, T. Akao, M. Hattori, T. Namba, Metabolism of drugs by intestinal bacteria, Bifidobacteria Microflora 11 (1992) 9–23.
[18] J.R. Saha, V.P. Butler Jr., H.C. Neu, J. Lindenbaum, Digoxin-inactivating bacteria: identification in human gut flora, Science 220 (1983) 325–327.
[19] T. Akao, H. Kida, M. Kanaoka, M. Hattori, K. Kobashi, Intestinal bacterial hydrolysis is required for the appearance of compound K in rat plasma after oral administration of ginsenoside Rb1 from Panax ginseng, J. Pharm. Pharmacol. 50 (1998) 1155–1160.
[20] G. Chen, M. Yang, Y. Song, Z. Lu, J. Zhang, H. Huang, S. Guan, L. Wu, D.A. Guo, Comparative analysis on microbial and rat metabolism of ginsenoside Rb1 by high-performance liquid chromatography coupled with tandem mass spectrometry, Biomed. Chromatogr. 22 (2008) 779–785.
[21] K. Kobashi, T. Akao, Relation of intestinal bacteria to phamacological effects of glycosides, Biosci. Microflora 16 (1997) 1–7.
[22] J. Lee, E. Lee, D. Kim, J. Yoo, B. Koh, Studies on absorption, distribution and metabolism of ginseng in humans after oral administration, J. Ethnopharmacol. 122 (2009) 143–148.
[23] M.A. Tawab, U. Bahr, M. Karas, M. Wurglics, M. Schubert-Zsilavecz, Degradation of ginsenosides in humans after oral administration, Drug Metab. Dispos. 31 (2003) 1065–1071.
[24] E.A. Bae, M.K. Choo, E.K. Park, S.Y. Park, H.Y. Shin, D.H. Kim, Metabolism of ginsenoside R(c) by human intestinal bacteria and its related antiallergic activity, Biol. Pharm. Bull. 25 (2002) 743–747.
[25] H.T. Xie, G.J. Wang, J.G. Sun, I. Tucker, X.C. Zhao, Y.Y. Xie, H. Li, X.L. Jiang, R. Wang, M.J. Xu, W. Wang, High performance liquid chromatographic–mass spectrometric determination of ginsenoside Rg3 and its metabolites in rat plasma using solid-phase extraction for pharmacokinetic studies, J. Chromatogr. B: Analyt. Technol. Biomed. Life Sci. 818 (2005) 167–173.
[26] T. Qian, Z. Cai, R.N. Wong, Z.H. Jiang, Liquid chromatography/mass spectrometric analysis of rat samples for in vivo metabolism and pharmacokinetic studies of ginsenoside Rh2, Rapid. Commun. Mass Spectrom. 19 (2005) 3549–3554.
[27] Y.W. Ha, Y.C. Na, J.J. Seo, S.N. Kim, R.J. Linhardt, Y.S. Kim, Qualitative and quantitative determination of ten major saponins in Platycodi Radix by high performance liquid chromatography with evaporative light scattering detection and mass spectrometry, J. Chromatogr. A 1135 (2006) 27–35.
[28] Y.C. Na, Y.W. Ha, Y.S. Kim, K.J. Kim, Structural analysis of platycosides in Platycodi Radix by liquid chromatography/electrospray ionization-tandem mass spectrometry, J. Chromatogr. A 1189 (2008) 467–475.
[29] M. Cui, F. Song, Z. Liu, S. Liu, Metal ion adducts in the structural analysis of ginsenosides by electrospray ionization with multi-stage mass spectrometry, Rapid Commun. Mass Spectrom. 15 (2001) 586–595.
[30] F. Song, M. Cui, Z. Liu, B. Yu, S. Liu, Multiple-stage tandem mass spectrometry for differentiation of isomeric saponins, Rapid Commun. Mass Spectrom. 18 (2004) 2241–2248.
[31] B. Domon, C.E. Costello, A systematic nomenclature for carbohydrate fragmentations in FAB-MS/MS spectra of glycoconjugates, Glycoconj. J. 5 (1988) 397–409.
[32] S. Broberg, L.I. Nord, L. Kenne, Oligosaccharide sequences in Quillaja saponins by electrospray ionization ion trap multiple-stage mass spectrometry, J. Mass Spectrom. 39 (2004) 691–701.
[33] D.C. van Setten, G.J. ten Hove, E.J. Wiertz, J.P. Kamerling, G. van de Werken, Multiple-stage tandem mass spectrometry for structural characterization of saponins, Anal. Chem. 70 (1998) 4401–4409.